Quantum Electronics **37** (3) 273 – 284 (2007)

SUPERSTRONG FIELDS

PACS numbers: 41.75.Jv;42.65.Re
DOI: 10.1070/QE2007v037n03ABEH013462

Acceleration of electrons by tightly focused femtosecond laser pulses

S.G. Bochkarev, V.Yu. Bychenkov

Abstract. **The problem of the acceleration of a test electron in the field of a tightly focused relativistic laser pulse is solved in the case when the focal spot size is of the order of the radiation wavelength and the exact solution of Maxwell's equations for the electromagnetic field should be used. The electron acceleration is studied depending on the initial position of the electron in the focal plane and is compared with the results corresponding to the paraxial approximation for the laser field. The maximum energy acquired by the electron in the laser focus is found. The dependences of the ejection angle of the electron on its initial position near the focus are analysed.**

Keywords: *short laser pulse, electron acceleration, tight focusing.*

1. Introduction

At present experimental studies of the interaction of relativistic laser pulses with matter attract great attention because high-power short-pulse lasers have become available in recent years. Hereafter, a laser pulse is called relativistic if an electron can acquire the relativistic energy in the pulse focus. It is obvious that the maximum intensity can be achieved when the laser pulse is very tightly focused on a target to produce the focal spot of size close to the diffraction limit. However, it is not definitely clear so far whether such tight focusing is optimal for the most efficient acceleration of particles in the laser focus. At present the focal spot size of the order of the laser wavelength was achieved [1 – 3]. The interaction between tightly focused laser radiation and a plasma is determined by a peculiar topology of the laser field in the focus, especially if we are dealing with nanotargets – ultrathin films, nanowires (nanotubes), nanospheres (nanoshells) or other more complicated nanoobjects of size much smaller than the laser wavelength. An example is the problem of the so-called vacuum acceleration of electrons, which was studied in many theoretical [4 – 15] and experimental [16 – 18] papers.

S.G. Bochkarev, V.Yu. Bychenkov P.N. Lebedev Physics Institute, Russian Academy of Sciences, Leninsky prosp. 53, 119991 Moscow, Russia; e-mail: bochkar@sci.lebedev.ru

Received 19 October 2006; revision received 12 January 2007
Kvantovaya Elektronika **37** (3) 273 – 284 (2006)
Translated by M.N. Sapozhnikov

The acceleration of particles from nanotargets irradiated by a tightly focused laser beam can be studied most completely by using a powerful modern numerical kinetic method, the so-called particle-in-cell (PIC) simulation. The PIC simulation is devoid of a number of simplifications inherent in idealised theoretical models. In the case of real three-dimensional geometry, it requires considerable computer resources, and it is natural that it is necessary to analyse the motion of a test particle in the laser focus before performing detail calculations. Note that analysis of the motion of test particles in the laser pulse field can quite accurately characterise the behaviour of the nanotarget as a whole if the energy acquired by electrons in the laser field greatly exceeds their Coulomb interaction energy.

At present the problem of the interaction of a test electron with the laser field is solved completely enough in the case when the field is described in the approximation of quasi-optics (paraxial approximation for a laser beam [19]). This interaction was studied in most papers on the acceleration of electrons by a localised laser field [4, 5, 8, 9, 11 – 15]. However, such an approach is not valid upon tight focusing, when the focal spot size proves to be comparable with the laser wavelength. The model was further refined by using the perturbation theory for the paraxial approximation [6, 10, 20 – 24] in the ratio of the wavelength λ to the focal spot radius ρ_F as a parameter. In addition, more sophisticated methods pretending to a more consistent description of the laser field in the focus were developed such as, for example, the model proposed in paper [7], where a more general class of solutions of Maxwell's equations describing a focused laser beam was found. However, this method is valid only if the condition $k\rho_F \gg 1$ is fulfilled, where $k = 2\pi/\lambda$ {see condition (2) in [7]}. This condition is not satisfied for tightly focusing systems of the type considered in [1 – 3]. For example, the focal spot radius for a Hercules laser [3] is equal approximately to half the wavelength. In this case, it is necessary to use exact solutions of Maxwell's equations, which has not been done so far for the description of the acceleration of a test particle. The solution of this problem is the aim of this paper. Note that the method for describing the laser field produced upon extremely tight focusing of the laser beam in experiments [3] was proposed in [25]. However, the authors of [25] did not pursue the goal to study the acceleration of particles in such a field.

A laser beam with a focusing radius exceeding the laser wavelength and with the intensity slowly varying in time (compared to the laser field period) can be treated in the zero approximation as a transverse plane electromagnetic

wave with a slowly varying amplitude, and the acceleration of electrons in this wave can be studied in the adiabatic approximation [26]. Due to slow variations in the laser radiation intensity, an electron is first accelerated at the leading edge of the laser pulse. After the interaction with the pulse, the electron loses the acquired energy due to its deceleration at the trailing edge of the pulse. As a result, in accordance with the so-called Lawson–Woodward theorem [5, 27, 28], the electron does not acquire energy. To accelerate the electron, it is necessary to violate the adiabaticity condition. This is possible for a laser pulse with high enough transverse gradients, which are produced, for example, upon focusing laser radiation to a spot of radius of a few wavelengths. Such a tight focusing can result in the loss of the adiabaticity and in the noticeable acceleration of electrons. The latter was recently observed in experiments [16–18]. In this case, the longitudinal component of the electric field produced due to radiation focusing cannot be neglected in the theoretical analysis [6, 10, 12–14, 21, 23, 29]. A consideration of the longitudinal field leads to substantial changes in the acceleration efficiency of particles even upon moderately tight focusing; however, this field was erroneously neglected in calculations until recently [4, 17]. The adiabaticity can be broken because the amplitude of transverse oscillations of electrons excited by tightly focused relativistic pulses can be comparable with the focal spot radius. It follows from the theory in this case that the electron that has acquired considerable energy can leave the region of the maximum intensity [4, 6, 8–10, 12–14].

By now numerous schemes have been developed for accelerating electrons by laser pulses, which are based on the breaking of the adiabaticity of this process, including effects of a strong nonstationarity of pulses and additional fields. For example, it was proposed to use laser pulses with sharply rising leading edges [30] or ultrashort pulses of duration of only a few optical cycles [31], beatings of electromagnetic waves with close frequencies [5], schemes with the acceleration of electrons in a preliminarily ionised plasma (produced, for example, by a weaker prepulse) [11], acceleration in the presence of a constant magnetic field [32], acceleration achieved by applying different modes (combined Gaussian beam) [8, 15], etc. Note that many of these schemes are difficult to realise. In particular, the scheme with a laser pulse with a steep leading edge [30] was not realised so far. At the same time, the preionisation method proposed in [11] can be used in experiments. Note that the idea of this method is close to that proposed in [30].

In this paper, we study the acceleration of a test electron in vacuum by using the exact solution of the Helmholtz equation, which describes a tightly focused light beam, and compare the results with the results obtained in the paraxial approximation. The acceleration of the electron is considered in the field of the laser pulse with the envelope symmetric in time and duration $\tau \gg T$, where T is the optical oscillation period in the case of the maximal focusing of the laser pulse, when the focal spot size proves to be of the order of the wavelength. We also investigate the acceleration of the test electron in a preliminarily ionised plasma. In this case, the acceleration begins near the maximum of the laser pulse (after ionisation). The efficiency and direction of electron acceleration are analysed depending on its initial position in the focal region and the phase of the accelerating field.

2. Solution of the wave equation

To construct the solution of Maxwell's equations in vacuum for the electromagnetic field of a focused laser beam

$$\begin{aligned} &\operatorname{div} \boldsymbol{B} = 0, \quad \operatorname{rot} \boldsymbol{E} = -\frac{1}{c}\frac{\partial \boldsymbol{B}}{\partial t}, \\ &\operatorname{rot} \boldsymbol{B} = \frac{1}{c}\frac{\partial \boldsymbol{E}}{\partial t}, \quad \operatorname{div} \boldsymbol{E} = 0 \end{aligned} \tag{1}$$

we will use the vector and scalar potentials $\boldsymbol{A}$ and Φ

$$\boldsymbol{E} = -\frac{1}{c}\frac{\partial \boldsymbol{A}}{\partial t} - \nabla\Phi, \quad \boldsymbol{B} = \operatorname{rot} \boldsymbol{A}, \tag{2}$$

satisfying the Lorentz gauge $\operatorname{div} \boldsymbol{A} + c^{-1}\partial\Phi/\partial t = 0$. Then, by following papers [15, 20], we will seek the solution of Eqns (1) for the polarised TM wave with the vector potential $\boldsymbol{A} = \{A_x \equiv A, 0, 0\}$ propagating in the direction z. In the case of smooth focusing (paraxial approach), the acceleration of the test electron by this wave was studied in most papers cited above, for example, in [10, 15]. Note that, although the choice of this mode corresponds to a particular case, it meets the aim of our paper to demonstrate the peculiarities of the acceleration of electrons in the diffraction limit, when the radiation intensity distribution in the focal region is strongly inhomogeneous.

Thus, to describe the propagation of a converging electromagnetic wave in a free space within the framework of our model, it is necessary to solve the scalar wave equation

$$\Delta A - \frac{1}{c^2}\frac{\partial^2 A}{\partial t^2} = 0. \tag{3}$$

The scalar potential Φ can be easily found from the gauge condition. In the case of the quasi-monochromatic electromagnetic field, the vector and scalar potentials can be represented in the form

$$\begin{aligned} A(t, \boldsymbol{R}) &= \operatorname{Re}\left[\hat{A}(t, \boldsymbol{R}) \exp(-\mathrm{i}\omega_0 t)\right], \\ \Phi(t, \boldsymbol{R}) &= \operatorname{Re}\left[\hat{\Phi}(t, \boldsymbol{R}) \exp(-\mathrm{i}\omega_0 t)\right], \end{aligned} \tag{4}$$

where $\boldsymbol{R} = \{x, y, z\}$ is the radius vector; and $\hat{A}(t, R)$ and $\hat{\Phi}(t, \boldsymbol{R})$ are slowly varying complex field amplitudes at the carrier frequency ω_0. Then, we have the Helmholtz equation

$$\Delta\hat{A} + k_0^2\hat{A} = 0 \tag{5}$$

for the complex amplitude of the vector potential, where $k_0 = \omega_0/c$. To find the solution of Helmholtz equation (5) from the given distribution $\hat{A}(\boldsymbol{r}, z = 0) = \hat{A}_0(\boldsymbol{r})$, where $\boldsymbol{r} = \{x, y\}$ in a plane $z = 0$ located in front of the focal plane, we expand this distribution in the Fourier integral

$$\hat{A}_0(\boldsymbol{r}) = \int_{-\infty}^{\infty}\int_{-\infty}^{\infty} \hat{A}_0(\boldsymbol{b}) \exp[\mathrm{i}k_0(px + qy)]\mathrm{d}p\mathrm{d}q, \tag{6}$$

where $\boldsymbol{b} = \{p, q\}$ is the dimensionless wave number. We will seek the complex amplitude of the vector potential $\hat{A}(\boldsymbol{r}, z)$ in the spatial region $z \geqslant 0$ in the form similar to (6)

$$\hat{A}(\boldsymbol{R}) = \int_{-\infty}^{\infty}\int_{-\infty}^{\infty} \hat{A}(\boldsymbol{b}, z)\exp[\mathrm{i}k_0(px+qy)]\mathrm{d}p\,\mathrm{d}q. \quad (7)$$

According to (5) and (7), the equation for the spectral amplitude $\hat{A}(\boldsymbol{b}, z)$ has the form

$$\frac{\partial^2\hat{A}}{\partial z^2} + k_0^2\left(1-b^2\right)\hat{A} = 0, \quad (8)$$

where $b = (p^2+q^2)^{1/2}$.

By introducing the dimensionless longitudinal wave number m, we write the solution of (8) as

$$\hat{A}(\boldsymbol{b}, z) = C_1\exp(\mathrm{i}mk_0z) + C_2\exp(-\mathrm{i}mk_0z), \quad (9)$$

where the value of m is defined, depending on the sign of $1-b^2$, as [6, 21]

$$m = (1-b^2)^{1/2}, \;\; b^2 \leqslant 1,$$
$$m = \mathrm{i}(b^2-1)^{1/2}, \;\; b^2 > 1. \quad (10)$$

Here, we select from possible solutions (9) the solution corresponding to the wave propagating at the speed of light along the positive direction of the z axis and satisfying the boundary condition considered for $z = 0$. Therefore, we set $C_2 = 0$ and $C_1 = \hat{A}_0(\boldsymbol{b})$ in (9). Note that the condition $b^2 > 1$ corresponds to non-propagating (evanescent) waves, which appear in the spatial spectrum upon focusing laser radiation into a spot of diameter of the order of the radiation wavelength. Unlike expressions in [6], the non-propagating waves are taken into account in the solution obtained. These waves can be neglected only under the condition $k_0\rho_\mathrm{F} \gg 1$ of smooth focusing.

By substituting (9) and (10) into (7), we can find $\hat{A}$ and, hence, the electric field strength and magnetic field induction because $\hat{\Phi} = -\mathrm{i}k_0^{-1}\partial\hat{A}/\partial x$. The complex amplitudes of the electric field strength and magnetic field induction $\hat{\boldsymbol{E}}(\boldsymbol{R})$ and $\hat{\boldsymbol{B}}(\boldsymbol{R})$ and these quantities themselves are determined by the relations

$$\hat{\boldsymbol{B}} = \left\{0, \frac{\partial\hat{A}}{\partial z}, -\frac{\partial\hat{A}}{\partial y}\right\}, \quad (11)$$

$$\hat{\boldsymbol{E}} = \left\{\mathrm{i}k_0\hat{A} - \frac{\partial\hat{\Phi}}{\partial x}, -\frac{\partial\hat{\Phi}}{\partial y}, -\frac{\partial\hat{\Phi}}{\partial z}\right\}, \quad (12)$$

$$\boldsymbol{B}(t,\boldsymbol{R}) = \mathrm{Re}\left[\hat{\boldsymbol{B}}\exp(-\mathrm{i}\omega_0 t)\right], \; \boldsymbol{E}(t,\boldsymbol{R}) = \mathrm{Re}\left[\hat{\boldsymbol{E}}\exp(-\mathrm{i}\omega_0 t)\right], \quad (13)$$

which are finally expressed in terms of function (9) specified by the field distribution at the input (for $z = 0$). For definiteness, we will consider below the case of the Gaussian laser radiation distribution and the convergence angle of its wavefront specified at the input. The latter is equivalent to the specification of the so-called f number or its inverse value called the aperture ratio [33]. Obviously, the results can be easily generalised to the case of an arbitrary axially symmetric laser radiation intensity distribution.

Taking into account the above said, we specify the distribution of the vector potential away from the focus (boundary condition) in the form

$$\hat{A}_0(r) \equiv \hat{A}(r, z=0) = A^0\exp\left(-\frac{\mathrm{i}k_0r^2}{4\rho_0 f}\right)\exp\left(-\frac{r^2}{2\rho_0^2}\right),$$
$$A^0 = |A^0|\exp(\mathrm{i}\varphi_0) = \mathrm{const}. \quad (14)$$

Here, $r = (x^2+y^2)^{1/2}$; ρ_0 is the beam radius; φ_0 is the wave phase for $z = 0$; f is the parameter determining of the convergence angle of the wave front, which is related in the quasi-optical approximation with the coordinate z_F of the focal plane (i.e the plane in which the beam radius $\rho = \rho_\mathrm{F}$ is minimal) by the expression $z_\mathrm{F} \approx 2\rho_0 f$. The choice of the dependence of the phase factor on r in (14) determines the converging wave front and corresponds to the standard formulation of the problem of light-beam focusing [19]. It is well known [34] that the real distance from the focus to a focusing system is somewhat smaller than $2\rho_0 f$, this difference increasing with decreasing the parameter $k_0\rho_0$. Note also that such a situation also takes place in the case of a paraxial beam [19].

The expression for spectral amplitude (9) for the initial distribution (14) in the region $z \geqslant 0$ takes the form

$$\hat{A}(b,z) = \frac{A^0}{2\pi\epsilon_0^2\alpha}\exp\left(-\frac{b^2}{2\alpha\epsilon_0^2}\right)\exp\left[\mathrm{i}(1-b^2)^{1/2}k_0z\right], b \leqslant 1,$$
$$\hat{A}(b,z) = \frac{A^0}{2\pi\epsilon_0^2\alpha}\exp\left(-\frac{b^2}{2\alpha\epsilon_0^2}\right)\exp\left[-(b^2-1)^{1/2}k_0z\right], b > 1, \quad (15)$$

where $\alpha = 1 + \mathrm{i}(2\epsilon_0 f)^{-1}$ and $\epsilon_0 = k_0^{-1}\rho_0^{-1}$. It is taken into account in (15) that for the input axially symmetric distribution $\hat{A}_0(r)$ considered here, the amplitude of the vector potential depends only on (r, z), while the spectral amplitude of the vector potential depends only on b and z. Then, by using expressions (7) and (15), passing to polar coordinates in the plane (p, q), and integrating over the polar angle, we obtain the expression for the complex amplitude of the vector potential

$$\hat{A}(r,z) = \int_0^1 Q_1(z,b)J_0(k_0rb)\mathrm{d}b + \int_1^\infty Q_2(z,b)J_0(k_0rb)\mathrm{d}b, \quad (16)$$

where

$$Q_1 = \frac{A^0 b}{\epsilon_0^2\alpha}\exp\left(-\frac{b^2}{2\alpha\epsilon_0^2}\right)\exp\left[\mathrm{i}(1-b^2)^{1/2}k_0z\right];$$
$$Q_2 = \frac{A^0 b}{\epsilon_0^2\alpha}\exp\left(-\frac{b^2}{2\alpha\epsilon_0^2}\right)\exp\left[-(b^2-1)^{1/2}k_0z\right];$$

and J_0 is the zero-order Bessel function of the first kind. The kernels Q_1 and Q_2 describe contributions from propagating and non-propagating waves, respectively.

By substituting $\hat{A}$ into (1), we obtain the components of the complex amplitudes of the magnetic field induction

$$\hat{B}_x = 0, \;\; \hat{B}_y = \mathrm{i}k_0\int_0^1 Q_1(1-b^2)^{1/2}J_0(k_0rb)\mathrm{d}b - k_0\int_1^\infty Q_2(b^2-1)^{1/2}J_0(k_0rb)\mathrm{d}b, \quad (17)$$
$$\hat{B}_z = \frac{k_0 y}{r}\left[\int_0^1 Q_1 bJ_1(k_0rb)\mathrm{d}b + \int_1^\infty Q_2 bJ_1(k_0rb)\mathrm{d}b\right],$$

where J_1 is the first-order Bessel function of the first kind. Similarly, according to (12), we have the components of the complex amplitudes of the electric field strength

$$\hat{E}_x = \mathrm{i}\int_0^1 Q_1\left\{\frac{bJ_1(k_0rb)}{r}+\frac{by^2}{r^3}\left[k_0rbJ_0(k_0rb)-2J_1(k_0rb)\right]\right.$$
$$\left.+k_0(1-b^2)J_0(k_0rb)\right\}\mathrm{d}b$$
$$+\mathrm{i}\int_1^\infty Q_2\left\{\frac{bJ_1(k_0rb)}{r}+\frac{by^2}{r^3}\left[k_0rbJ_0(k_0rb)-2J_1(k_0rb)\right]\right.$$
$$\left.+k_0(1-b^2)J_0(k_0rb)\right\}\mathrm{d}b, \qquad (18)$$
$$\hat{E}_y = \frac{\mathrm{i}xy}{r^3}\left\{\int_0^1 Q_1 b\left[2J_1(k_0rb)-k_0rbJ_0(k_0rb)\right]\mathrm{d}b\right.$$
$$\left.+\int_1^\infty Q_2 b\left[2J_1(k_0rb)-k_0rbJ_0(k_0rb)\right]\mathrm{d}b\right\},$$
$$\hat{E}_z = \frac{k_0x}{r}\left[\int_0^1 Q_1 b(1-b^2)^{1/2}J_1(k_0rb)\mathrm{d}b\right.$$
$$\left.+\mathrm{i}\int_1^\infty Q_2 b(b^2-1)^{1/2}J_1(k_0rb)\mathrm{d}b\right].$$

Expressions (17) and (18) determine the configuration of the electromagnetic field in the laser beam without the assumption that the value of $k_0\rho_\mathrm{F}$ is large, which is used in the paraxial approximation. The structure of fields in the vicinity of the focus in the case of tight focusing is considered below in section 3.

In the case of smooth focusing ($k_0\rho_\mathrm{F} \gg 1$), integral (16) can be considerably simplified. In this case, the angular radiation spectrum is narrow because $k_\perp \ll k_0$, where $k_\perp = (k_x^2+k_y^2)^{1/2}$, and because $k_\perp \sim \rho^{-1} < \rho_\mathrm{F}^{-1}$, only the region of small values of $b = k_\perp/k_0 \ll 1$ makes the main contribution to integral (16). Then, we obtain from (16) the approximate expression for the vector potential

$$A_x(t,r,z) = |A^0|\frac{\rho_0}{\rho(z)}\exp\left[-\frac{r^2}{2\rho^2(z)}\right]\cos[\varphi(t,r,z)],$$
$$\varphi = \omega_0 t - k_0 z + \arctan\left[\frac{zz_*^{-1}}{1-z(2\rho_0 f)^{-1}}\right] + \pi\theta(z-2\rho_0 f)$$
$$-\frac{zr^2\left[1+z_*^2/(2\rho_0 f)^2-(2z\rho_0 f)^{-1}z_*^2\right]}{2z_*\rho^2(z)} - \varphi_0, \qquad (19)$$
$$\rho(z) = \rho_0\left[\left(1-\frac{z}{2\rho_0 f}\right)^2+\frac{z^2}{z_*^2}\right]^{1/2},$$

where $z_* = k_0\rho_0^2$ and $\theta(z)$ is the Heaviside function. This expression corresponds to the so-called paraxial approximation or quasi-optics approximation, which is widely used to describe the propagation of laser beams [19].

Expression (19) gives the following expressions for the electric field strength and magnetic field induction:

$$B_x = 0, \quad B_y = \frac{k_0|A^0|\rho_0}{\rho(z)}\exp\left[-\frac{r^2}{2\rho^2(z)}\right]\sin\varphi,$$
$$B_z = \frac{\epsilon(z_\mathrm{F})k_0|A^0|y\rho_0}{\rho^2(z)}\exp\left[-\frac{r^2}{2\rho^2(z)}\right]\cos\varphi_1, \; E_x = B_y, \; E_y = 0,$$
$$E_z = \frac{\epsilon(z_\mathrm{F})k_0|A^0|x\rho_0}{\rho^2(z)}\exp\left[-\frac{r^2}{2\rho^2(z)}\right]\cos\varphi_1, \qquad (20)$$
$$\varphi_1 = \varphi + \arctan\left[\frac{z}{z_*-zz_*(2\rho_0 f)^{-1}}\right] - \arctan\left(\frac{z_*}{2\rho_0 f}\right),$$
$$\epsilon(z_\mathrm{F}) = k_0^{-1}\rho_\mathrm{F}^{-1}, \quad z_\mathrm{F} = \frac{2\rho_0 f}{1+(2\rho_0 f)^2 z_*^{-2}},$$

where $\epsilon(z_\mathrm{F}) \ll 1$. Note that the use of boundary condition (14) in the paraxial limit here can be interpreted as the specification of a Gaussian beam with the wave front corresponding to its focusing by a thin lens [19].

Expressions (16)–(20) can be used in the case of the slow varying amplitude of the vector potential represented in the form $A^0 = A^0(z-ct)$ [6]. Such a quasi-stationary model describes the specified shape of a pulse characterised by the time scale τ greatly exceeding the laser wave period ($\omega_0\tau \gg 1$). In this case, the condition $c\tau \gg \rho(z_\mathrm{F})$ also should be fulfilled [6, 7]. If these inequalities are violated, it is necessary to seek a rigorous analytic solution of Eqn (3), whereas here we restrict our consideration to the quasi-stationary model.

3. Structure of the electromagnetic field in the case of tightly focused laser radiation

When an electromagnetic pulse is tightly focused to the region of size comparable with the radiation wavelength, the structure of the field changes noticeably compared to that in the case of smooth focusing described by the paraxial approximation. This in turn changes the type of acceleration of electrons. To interpret the results of numerical simulation of the acceleration of electrons, we consider first of all the laser field structure near the focus. The numerical study of the field and trajectories of electrons was performed by using the Mathematics applied software package [35]. Hereafter, k_0^{-1}, ω_0^{-1}, and $E_* = m_\mathrm{e}c\omega_0/e$ (where m_e and e are the electron mass and charge) are used as the units of length, time, and electric field strength. For definiteness, we will use the parameters $\lambda = 0.8$ μm and $\rho_\mathrm{F} = 0.45\lambda$ of the laser setup described in [3]. We also assume that $f = 0.5$ and $\epsilon_0 = 0.01$. According to our calculations, the value $k_0 z_\mathrm{F} \approx 82$ corresponds to these values.

Figure 1 presents the spatial distributions of quantities $|\hat{E}_x|^2$, $|\hat{E}_y|^2$, $|\hat{E}_z|^2$, $|\hat{B}_y|^2$, and $|\hat{B}_z|^2$ in the focal plane. The physical sense of the squares of moduli of the complex amplitudes is that the value $|\hat{E}_x|^2$, for example, is related to the value $|E_x|^2$ averaged over the light wave period by the expression $\langle E_x^2\rangle = |\hat{E}_x|^2/2$, where the angle brackets denote the time averaging. Note that the distribution of $|\hat{E}_x|^2$ in the focal plane for the selected parameters is anisotropic (Fig. 1a). However, according to (20), this anisotropy disappears in the paraxial limit, when $\hat{E}_x = \hat{B}_y$ and $\hat{E}_y = 0$, which means that radiation is linearly polarised in the focal plane. This fact already demonstrates that the

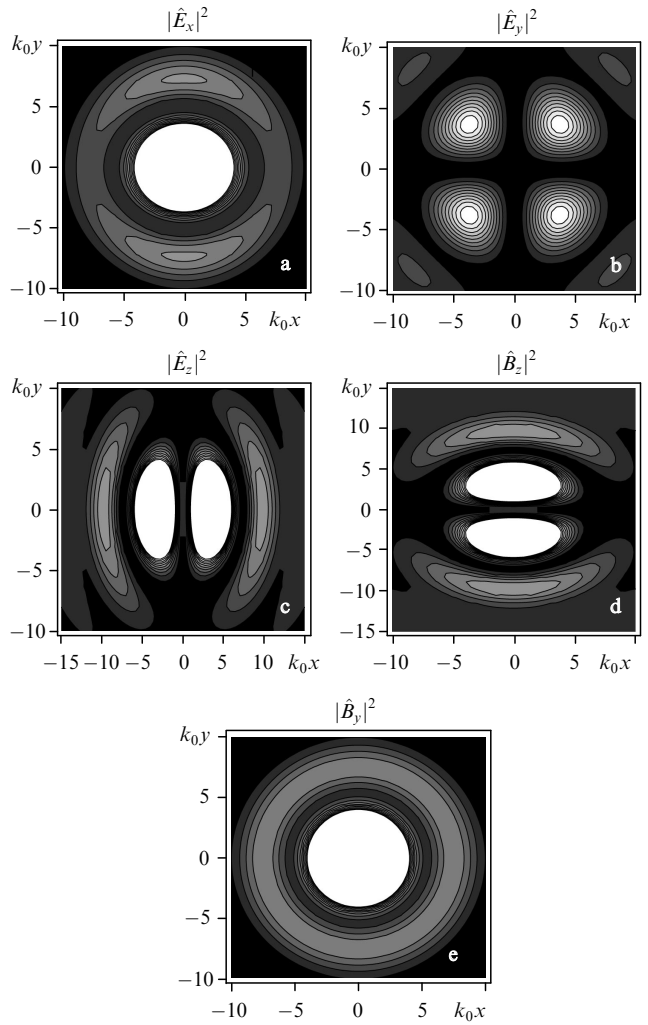

Figure 1. Distributions $|\hat{E}_x|^2$, $|\hat{E}_y|^2$, $|\hat{E}_z|^2$, $|\hat{B}_z|^2$, and $|\hat{B}_y|^2$ in the focal plane calculated by expressions (17) and (18) for $k_0\rho_F = 2.83$.

difference of the distribution of the laser field from the 'paraxial' distribution in this case is quite substantial and is explained in turn by the fact that the value of ϵ is not small [$\epsilon(z_F) = 0.35$]. As in the paraxial approximation, the distribution of $|\hat{B}_y|^2$ (Fig. 1e) is isotropic according to (17).

Figures 1c, d demonstrate the anisotropy of distributions of $|\hat{E}_z|^2$ and $|\hat{B}_z|^2$ in the focal plane. It follows from expressions (20) (paraxial approximation) that longitudinal fields have a similar but not equivalent anisotropy in the focal plane. In this case, in the paraxial approximation ($k_0\rho_F \gg 1$) the components $\hat{E}_z$ and $\hat{B}_z$ are negligibly small compared to $\hat{E}_x$. Figure 1b shows the distribution of $|\hat{E}_y|^2$ in the focal plane. One can see that the maxima of $|\hat{E}_y|^2$ are displaced from the z axis, as in the case of the longitudinal components $|\hat{E}_z|^2$ and $|\hat{B}_z|^2$. The maxima of distributions $|\hat{E}_z|^2$ and $|\hat{B}_z|^2$ in the paraxial approximation for the same laser spot radius are also displaced from the z axis but are located closer to it. Thus, for $\rho_F = 0.45\lambda$, the distance between the axis and maxima is less by half than it follows from expressions (17) and (18). Note that the longitudinal components of the fields upon tight focusing are not small and their influence on the acceleration of charged particles should be consistently taken into account. Because of the anisotropy of E_z and B_z in the plane $z = z_F$, the transverse components of the Lorentz force will also have the transverse anisotropy. Therefore, it should be expected that electrons located at the initial instant in the focal plane at the same distance from the z axis will be accelerated differently (see section 4).

Let us also discuss the distribution of the modulus of the Poynting vector $\boldsymbol{S}$, and first of all the anisotropy of the distribution, which follows from the exact solution (17), (18). The value of $|\boldsymbol{S}|$ is related to the electric field strength and magnetic field induction by the expression

$$|\boldsymbol{S}| = \frac{c}{8\pi}\Big\{\left[\mathrm{Re}(\hat{E}_y\hat{B}_z^* - \hat{E}_z\hat{B}_y^*)\right]^2 + \left[\mathrm{Re}(\hat{E}_z\hat{B}_x^* - \hat{E}_x\hat{B}_z^*)\right]^2 + \left[\mathrm{Re}(\hat{E}_x\hat{B}_y^* - \hat{E}_y\hat{B}_x^*)\right]^2\Big\}^{1/2}. \quad (21)$$

A specific feature of solution (17), (18) is that the coordinate $z = 2\rho_0 f$ of the focal plane decreases by $\sim 3\lambda$ compared to the paraxial case. Figure 2 presents the transverse and longitudinal distributions of $|\boldsymbol{S}|$ compared to the paraxial case corresponding to (20). Thus, the transverse distribution calculated from expressions (17) and (18) is virtually symmetric, as follows from Fig. 2a. For comparison, Fig. 2b demonstrates the transverse distribution of $|\boldsymbol{S}|$ for the focal spot of the same radius ($\rho_F = 0.45\lambda$) obtained by expressions (20) of the paraxial approximation, i.e. outside the framework of its application. Here, the value of ρ_F corresponds to the decrease in the value of $|\boldsymbol{S}|$ by a factor of e. In the case of tight focusing (Figs 2c, d), the distributions of $|\boldsymbol{S}|$ are substantially different: the distribution of $|\boldsymbol{S}|$ exhibits oscillations in front of the focal plane in Fig. 2c, whereas such oscillations are not observed in the paraxial case in Fig. 2d. The control calculation for the case $\epsilon(z_F) \ll 1$ showed good agreement between the field distributions obtained from (20) and calculated by expressions (17) and (18).

4. Acceleration of a test electron by a short laser pulse

We will describe the motion of an electron in the field of a tightly focused laser pulse with the symmetric envelope by assuming in (16) that

$$A^0 = A_0\exp(\mathrm{i}\varphi_0)\theta\left(1 - \frac{\sigma}{\omega_0\tau}\right)\theta\left(1 + \frac{\sigma}{\omega_0\tau}\right)\cos^2\left(\frac{\pi}{2}\frac{\sigma}{\omega_0\tau}\right),$$

$$\sigma = k_0z - \omega_0t + \omega_0\tau. \quad (22)$$

Here, we have a slowly varying function of the variable $k_0z - \omega_0t$ instead of $A^0 = \mathrm{const}$ in (14) and (16). The expression for the envelope A^0 was chosen in accordance with [4, 6]. Expression (22) corresponds to a laser pulse of duration τ. It is assumed below that the initial position of the electron is specified by the radius vector $\boldsymbol{R}_0 = \{x_0, y_0, z_0\}$. We assume that the laser pulse duration (FWHM) is ~ 30 fs, as for the laser used in [3], and $a = 100$, where $a = E_x^{\max}/E_*$, and $E_x^{\max}$ is the maximum value of E_x in the focus. This corresponds to the energy flux density at the maximum $m_e\omega_0^2c^3a^2/(8\pi e^2) \approx 2\times10^{22}$ W cm^{-2}. This value has been already achieved in experiments [3].

The evolution of the electron motion is described by the Lorentz equations

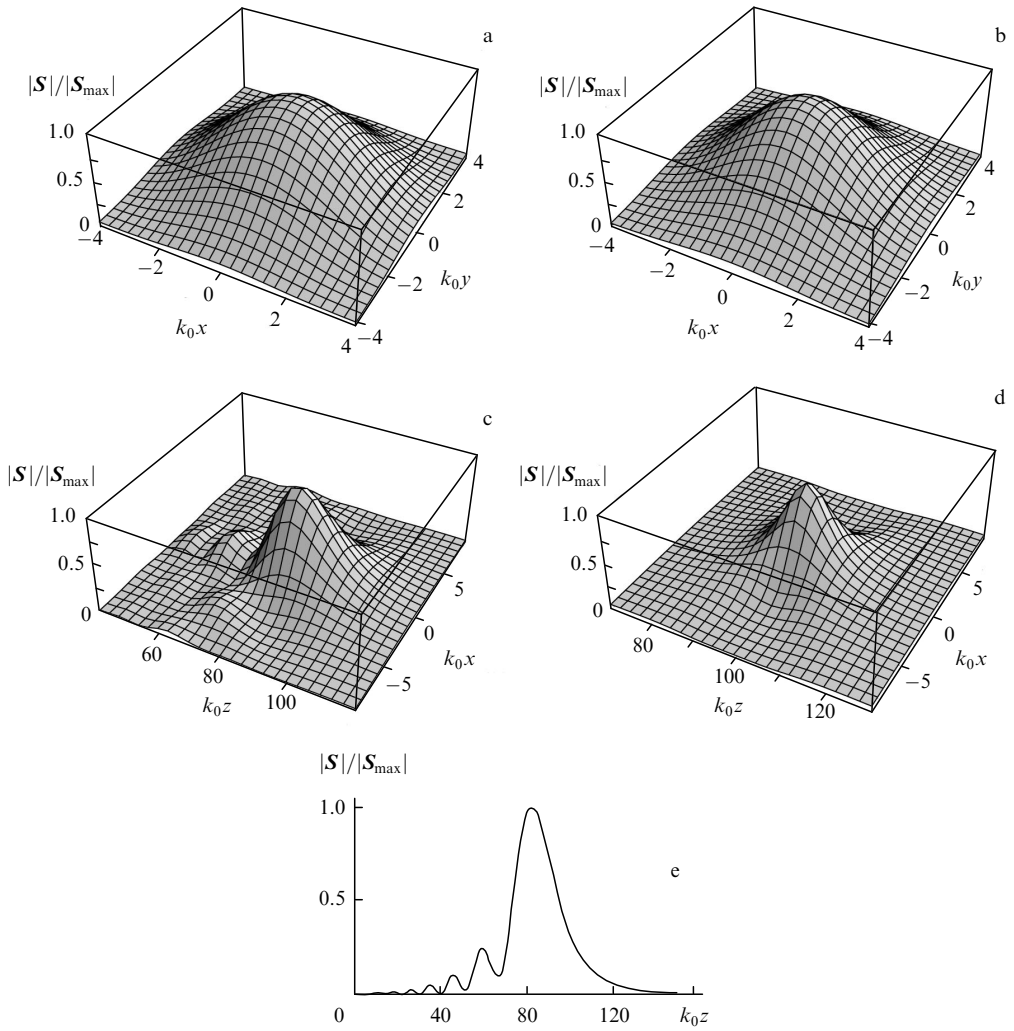

Figure 2. Distribution of the modulus of the Poynting vector in the x, y plane and the corresponding longitudinal-transverse distributions of $|\boldsymbol{S}|$ in the x, y plane calculated by exact expressions (17), (18), and (21) (a, c) and by paraxial expressions (20) and (21) (b, d) for the focal spot of the same size $k_0\rho_F = 2.83$; (e) distribution of $|\boldsymbol{S}|$ on the z axis.

$$\frac{\mathrm{d}\boldsymbol{p}}{\mathrm{d}t} = \boldsymbol{F}_E + \boldsymbol{F}_B,\ \boldsymbol{F}_E = -e\boldsymbol{E},\ \ \boldsymbol{F}_B = -\frac{e}{c}\boldsymbol{v}\times\boldsymbol{B},$$

$$\frac{\mathrm{d}\boldsymbol{R}}{\mathrm{d}t} \equiv \boldsymbol{v} = \frac{\boldsymbol{p}}{\gamma m_e},\ \ \gamma = \left(1 + \frac{\boldsymbol{p}^2}{m_e^2 c^2}\right)^{1/2}, \qquad (23)$$

where $\boldsymbol{v}$, $\boldsymbol{p}$, and $\gamma - 1$ are the electron velocity, momentum, and kinetic energy (in the units of $m_e c^2$); $\boldsymbol{F}_E$ is the force acting on the electron from the electric field; and $\boldsymbol{F}_B$ is the force acting on the electron from the magnetic field ($\boldsymbol{v}\times\boldsymbol{B}$ force). We will study the acceleration of the test electron for its several initial positions: the electron in the focal plane ($z_0 = z_F$), in front of the focal plane ($z_0 < z_F$), and behind the focus ($z_0 > z_F$). As follows from the study performed below, the electron energy and the ejection angle of the electron from the focal plane can strongly depend on its initial position.

For definiteness, we set the initial phase equal to $\varphi_0 = 0$ and consider first of all the situation when the electron is initially located in the focal plane. Consider three variants: (i) the electron is located exactly in the focus, i.e. its initial position is determined by the vector $\boldsymbol{R}_0 = \{0, 0, z_F\}$; (ii) the electron is displaced with respect to the focal-spot centre along the x axis parallel to the polarisation vector $\boldsymbol{A}$, $\boldsymbol{R}_0 = \{\lambda/2, 0, z_F\}$; and (iii) the electron is displaced along the y axis perpendicular to the polarisation vector, $\boldsymbol{R}_0 = \{0, \lambda/2, z_F\}$. Figure 3 presents the time evolution of γ and the electron momentum components. One can see that the electron very quickly, during a few optical cycles ($T = 2\pi/\omega_0$) acquires the relativistic energy. Then, being somewhat decelerated and again acquiring energy, the electron escapes from the strong-field region and flies freely from the focus. The characteristic acceleration time for variants i – iii, i.e. the time during which the electron acquires half its maximal energy is approximately 110, 20, and 110 fs, respectively. Note that the electron acquires the minimal energy in variant (ii), but its acceleration time is also minimal in this case. In the case of variants (i) and (ii), the electron always moves in the (x, z) plane and is only slightly displaced along the y axis ($p_y \approx 0$), whereas in variant (iii) the electron escapes with the large momentum component p_y comparable with p_x and p_z. In all the three cases, the angles of deviation of the electron ($\psi = \boldsymbol{p}\hat{}\boldsymbol{p}_z$) from the propagation direction of the light pulse (ejection angles) are large. Thus, these angles for variants (i), (ii), and (iii) are approximately 30°, 45°, and 45°, respectively. The rate of energy gain is maximal for variant (iii) ($\sim$135 GeV m^{-1}) and minimal for variant (ii) ($\sim$28

GeV m^{-1}), while this rate for variant (i) is $\sim$90 GeV m^{-1}. The rate of energy accumulation is defined here as $(\gamma-1)/|\boldsymbol{R}-\boldsymbol{R}_0|$, where $\gamma-1$ and $|\boldsymbol{R}-\boldsymbol{R}_0|$ are the finite kinetic energy in units of $m_e c^2$ and the approximate distance propagated by the electron before it begins to move by inertia. Thus, the rate of energy gain and the energy itself imparted to the electron located exactly at the laser focus prove to be far from maximal. In variant (iii), the electron acquires the maximum energy for the time $\sim$250 fs, which corresponds to $\gamma \approx 22$. In addition, the total acceleration time of the electron located initially at the focus [variant (i)], i.e. the time during which it passes to the inertial motion, exceeds acceleration times for variants (ii) and (iii) and is equal to $\sim$500 fs.

We can conclude as a whole that accelerated electrons escape at large angles to the z axis. This occurs because the longitudinal and transverse components of forces $\boldsymbol{F}_E$ and $\boldsymbol{F}_B$ are of the same order of magnitude. The parameters of escaping electrons (the ejection angle and energy) depend substantially on the initial position of the electron in the focal plane specified by the electron displacement from the focus by the distance of the order of the wavelength only. This is related to the extremely tight focusing of the laser pulse, which causes a strong dependence of the parameters of the accelerated electron on its initial position near the focus. In particular, Fig. 3 demonstrates a considerable difference between the energies of the accelerated electron displaced parallel to the polarisation vector (along the x axis) or perpendicular to it (along the y axis).

According to the simplest concepts about the motion of an electron in the field of a plane electromagnetic wave [26], the maximal energy of the electron should be quite high, $\gamma \sim a^2/2$. For the example discussed here, the electron energy is $\sim$2.5 GeV. However, the energy acquired by the electron proves to be approximately 200 times lower. The reason is that the electron accelerated at the leading edge of the pulse rapidly leaves the focal region before being subjected to the field at the pulse maximum. The study of the electron acceleration in the laser field in the paraxial approximation [6] has shown that the electron does not accumulate the energy $\sim a^2/2$, and this value is only the upper bound.

At the same time, the paraxial approach (for the focal spot of the same size and the same focal intensity of laser radiation) also gives the overestimated maximum energy of the electron leaving the focal region. If the electron located initially in the focal region accumulates the maximum energy $\gamma \approx 25$, the paraxial approximation gives in this case the maximum energy that is approximately an order of magnitude higher. Thus, the paraxial approximation in the case of very tight focusing considerably overestimates the real maximum energy of accelerated electrons. At the same time, when the pulse radiation is defocused, the acceleration efficiency can be higher, i.e. the electron energy can be noticeably higher in the case of smooth focusing than for very tight focusing for the same laser energy (this situation is considered below). For example, the energy $\gamma = 18$ for the electron located initially at the focus can be achieved by defocusing the laser pulse to $\rho_F = 5.5\lambda$, when the radiation intensity at the focus (1.5×10^{20} W cm^{-2}) proves to be much lower than upon tight focusing.

Figure 4 presents the dependences of the energy and ejection angle of the electron on its initial position in the focal plane calculated for the initial positions of the electron on the x and y axes. A comparison of these dependences with the corresponding dependences related to acceleration in 'paraxial' fields (20) demonstrates considerable differences both in electron energies and ejection angles. Calculations show that the electron energy and ejection angle depend nonmonotonically on the initial position of the

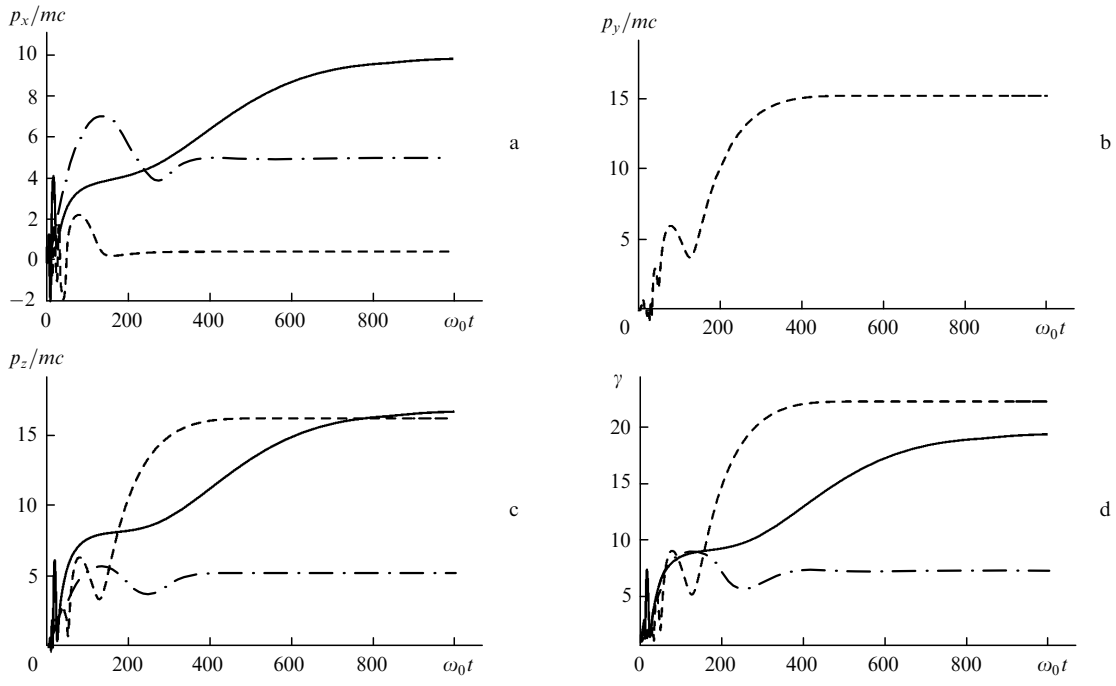

Figure 3. Evolution of the momentum components (a, b, c) and γ (d) for an electron accelerated in fields (17), (18) for the initial position of the electron determined by variants (i)–(iii) for symmetric laser pulse of duration $\sim$30 fs (22) with $a = 100$ and $k_0\rho_F = 2.83$. The solid, dot-and-dash, and dashed curves corresponds to variants (i), (ii), and (iii), respectively.

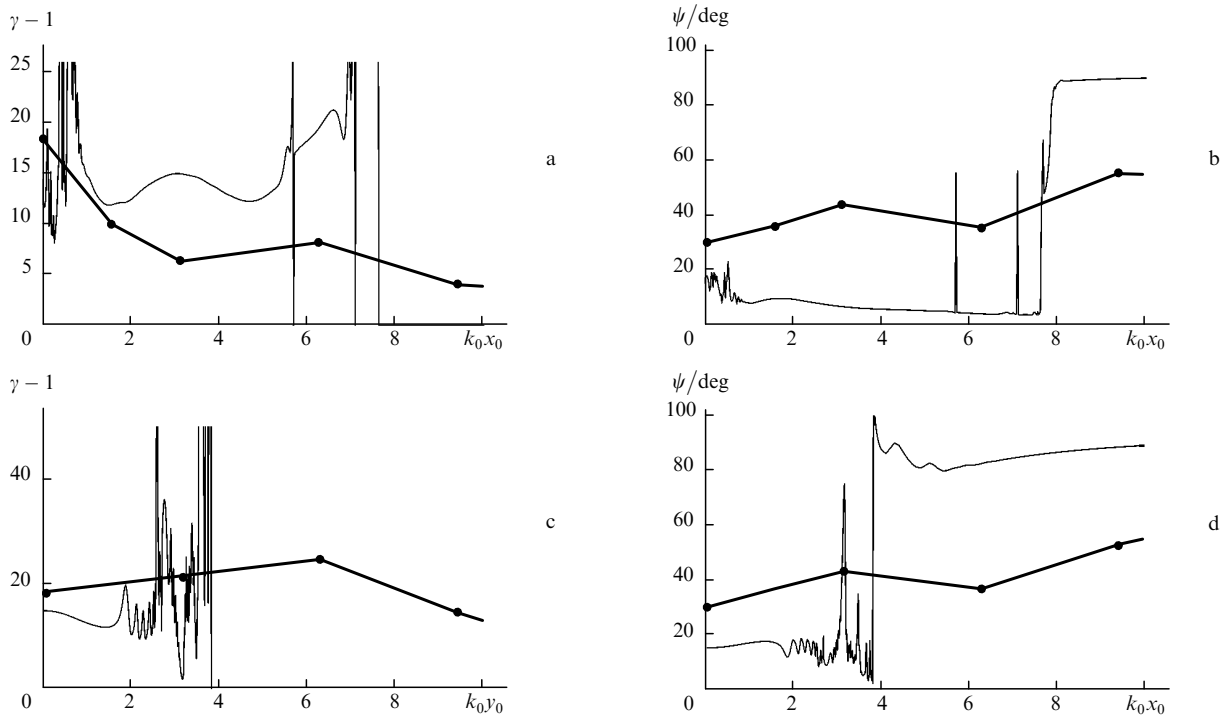

Figure 4. Dimensionless kinetic energy of the electron (a) and the angle of its ejection ψ (b) for a symmetric pulse as functions of the electron position x_0 in the focal plane on the x axis and the same dependences for electrons located on the y axis (c, d) (solid curves); thin curves correspond to the electron acceleration in paraxial fields (20). The laser pulse parameters are as in Fig. 3.

electron in the focal plane. This corresponds qualitatively but not quantitatively to the results of the paraxial approach. These effects are related to the tight focusing of radiation and demonstrate once more the influence of the longitudinal field components E_z and B_z on the electron acceleration. Longitudinal fields in (17), (18), and (20) have strongly anisotropic distributions in the focal plane, which leads to the anisotropic distribution of the electron escape parameters γ, ψ.

As a whole, the following behaviour is observed: moving away from the laser beam axis after acceleration in the focal plane, the electron escapes at a larger angle, as in the case of 'paraxial' fields, although this dependence is nonmonotonic. Note that, as the electron moves away from the beam axis in the direction parallel to the polarisation vector, the energy acquired by it decreases, while in the case of the electron departure from the beam axis in the direction perpendicular to the polarisation vector, the electron energy increases. It is natural that in the periphery region the electron energy decreases as the electrons moves away from the beam axis, independently of its initial position due to a drastic decrease in the laser radiation intensity in this region. If the electron is initially located in the polarisation plane, it remains in this plane during acceleration, which is typical for the paraxial approximation.

However, the situation is different for electrons initially located on the y axis. Being accelerated, these electrons escape at different angles to the polarisation plane. This differs substantially from acceleration in 'paraxial' fields for $k_0\rho_F \gg 1$, when the longitudinal fields E_z and B_z can be approximately neglected. In this case, the electron moves only in the plane parallel to the polarisation plane. However, the neglect of the longitudinal electric and magnetic field components, which was used in the simplest approaches in the case of not too smooth focusing, for example, in [4, 7], leads to incorrect results.

As a whole, the nonmonotonic dependences of γ on x_0 and y_0 prove to be quite smooth, unlike the dependences obtained in the paraxial approximation. The unjustified application of paraxial expressions when the strong inequality $k_0\rho_F \gg 1$ is violated can lead to quite unusual dependences of the electron energy and ejection angle on the initial electron position in the focal plane, in particular, sharp maxima (spikes) in the distribution of γ and ψ can be observed at some initial electron positions (Fig. 4). This clearly demonstrates the incorrectness of using paraxial expressions when the strong condition $k_0\rho_F \gg 1$ is not satisfied.

The size of the focal spot, from which the electron escapes by accumulating the relativistic energy in paraxial fields, proves to be smaller than in the case of the correct description of the acceleration of electrons in exactly defined fields (Figs 4a, c). The reason is that the paraxial approximation does not take diffraction effects into account correctly enough, thereby predicting a stronger localisation of the strong longitudinal field in the axial region than it follows from the exact theory. Note that the average energy of accelerated electrons initially located on the x axis proves to be overestimated when paraxial fields are used, while the average energy of accelerated electrons initially located on the y axis is approximately the same as in the case of exactly defined fields. Although the paraxial approach overestimates the maximum electron energy, it should be expected that the total number of electrons accelerated in the focal region, for example, up to relativistic energies will be greater in the case of exactly defined fields due to inaccurate consideration of diffraction effects in the paraxial approximation mentioned above.

Our study shows that the parameters γ and ψ are not strictly correlated for $k_0\rho_F \gtrsim 1$. Such a correlation is typical for the description of electrons moving in the case of smooth focusing ($k_0\rho_F \gg 1$) in the quasi-plane wave approximation, when $\cos\psi \simeq [(\gamma-1)/(\gamma+1)]^{1/2}$. The correlation is broken with decreasing the focal-spot radius, as was already demonstrated in the paraxial approximation [6, 14]. In the case of tight focusing, the violation of the correlation is even more pronounced. The absence of the correlation is demonstrated, for example, by a comparison of the two cases corresponding to the initial positions of the electron $\boldsymbol{R}_{01}=\{0,\lambda/4,z_F\}$ and $\boldsymbol{R}_{02}=\{0,0,z_F+\lambda/2\}$. In both cases, the energy $\gamma_{1,2}$ of electrons escaping from the focal region achieves ~ 10. At the same time, the ejection angles are substantially different ($\psi_1 \approx 50^\circ$ and $\psi_2 \approx 20^\circ$), whereas $\psi \approx 25^\circ$ according to expression (49) from [6].

Strictly speaking, the conclusions made above concern the case of an electron located initially in the focal plane. We also studied the acceleration of an electron located initially in planes lying both in front of the focal plane ($z_0 < z_F$) and behind it ($z_0 > z_F$) at distances of the order of the wavelength. It was found that the electron was still accelerated inefficiently. The general tendency is, however, that the maximum energy accumulated by the electron located in front of the focal plane proves to be somewhat higher than in the case of the initial location of the electron behind the focal plane. This conclusion is independent of the choice of the initial phase [$\varphi_0 \neq 0$ in (22)]. This effect is explained by the fact that the electron located initially in front of the focal plane is subjected to strong accelerating fields for a longer time because it is pushed forward to the focal region by the longitudinal component of the force $\boldsymbol{F}_B$. If the electron is located initially behind the focal plane, it is accelerated by weaker fields. The optimal position of the electron in front of the focus on the z axis corresponds to the condition $z_F - z_0 \approx 1.5\lambda$; in this case, $\gamma \approx 28$. Note, however, that the coordinate of the optimal position of the electron and its maximum energy vary somewhat depending on the initial phase of the field, but the position in front of the focal plane is always optimal. The same situation takes place qualitatively when paraxial fields with the same focal intensity and focusing radius are used. The optimal position of the electron in this case is determined by the condition $z_F - z_0 \approx 1.5\lambda$, and the electron energy is $\gamma \approx 200$, which considerably exceeds the energy accumulated by the electron.

To find the optimal focusing conditions providing the maximal acceleration of electrons for the specified laser energy ($a\rho_F = \text{const} = 45\lambda$), we performed calculations for different values of ρ_F in the range between $(0.5-20)\lambda$. In fact, we are dealing with the defocusing of laser radiation with the parameters $\rho_F = 0.45\lambda$ and $a = 100$ used above. We found that the maximum energy of the electron located exactly at the focus is a nonmonotonic function of the focal-spot radius. The optimal value of the radius is $\rho_F \approx 3.5\lambda$ ($a \approx 13$), to which the maximum energy $\gamma \approx 30$ of the accelerated electron corresponds. As the focal-spot radius is increased compared to its optimal value, the final electron energy decreases, as would be expected, and the electron accumulates no energy in the plane wave limit ($k_0\rho_F \gg 1$). For small focal-spot radii ($\rho_F \leqslant 3.5\lambda$), the energy of the accelerated electron increases with increasing ρ_F. Thus, for the electron located in the focal plane, the case of moderately tight focusing ($k_0\rho_F > 1$) is optimal. It should be emphasised that because the energy accumulated by the electron depends on its initial position, as shown above, the optimal focusing conditions for different positions of the electron with respect to the focal plane will be different.

A series of calculations of the electron acceleration performed for different values of φ_0 shows the noticeable dependence of the parameters of the accelerated electron on φ_0, although it does not demonstrate the qualitative difference from the results presented above for $\varphi_0 = 0$. A similar dependence was obtained in [36], where the electron motion was described in the paraxial approximation. For example, the energy of the electron located initially in the focal plane varies depending on the phase in the interval 13–18, i.e. within 30 %. If the initial position of the electron is displaced by the distance $\lesssim\lambda$ from the focal plane, variations in the electron energy depending on the initial phase are also moderate, lying within 30 %–40 %. If the electron is initially located on the laser beam axis, the dependence of the electron energy on the initial phase for a fixed position z_0 is periodic with the period π. This period is not equal to 2π, as could appear at first glance, because only the sign of p_x changes when the phase changes by γ, whereas the value of φ_0 remains invariable. The electron energy averaged over φ_0 as a function of the coordinate z_0 achieves its maximum $\gamma \simeq 18$ for $z_F - z_0 \simeq \lambda$.

5. Acceleration of the test electron by a laser pulse in a preliminarily ionised plasma

As mentioned in Introduction, a challenging idea for obtaining high-energy electrons is to use plasmas with highly charged ions as a target [11]. The plasma can be produced with the help of a prepulse whose intensity is insufficient to ionise the medium completely. The main, more intense pulse is used to further ionise plasma by producing electrons which are accelerated under the action of the central part of the laser pulse (near its maximum) rather than of its leading edge. This is explained by the fact that the atomic potential coupling electrons with a nucleus in highly charged ions will prevent ionisation until the laser field strength exceeds the threshold of the tunnel ionisation of the ion [37]. Free electrons will be initially subjected to almost the peak accelerating field, by accumulating a high energy before leaving the focal region. In this case, the acceleration efficiency can be substantially increased compared to the case considered in section 4, when the electron escaped from the focal region before the appearance of a strong field in it.

Thus, by using preliminarily ionised plasmas with highly charged ions, it is possible to increase the electron energy upon tight focusing. In fact, the problem of the acceleration of the test electron in preliminarily ionised plasmas is reduced to the problem of the electron acceleration by the field of a laser pulse with a steep leading edge [30].

We consider in this section the acceleration of an electron in the field of a laser pulse of the same shape (22) and duration and intensity as in section 4. The electron begins to move when it is already located in the laser pulse field $E = (E_x^2 + E_y^2 + E_z^2)^{1/2} = E_{th}$ that increased to the value sufficient to ionise the given ion, which is assumed to have a high degree of ionisation Z. The threshold radiation intensity required to perform the tunnelling ionisation of the ion is proportional to U_{ion}^4/Z^2, where U_{ion} is the ionisation potential. As an example, we consider

the acceleration of an electron produced upon photoionisation of Ti^{20+} ion in the laser field with $E > E_{th} \approx 71E_*$. To obtain a plasma with the Ti^{20+} ions, it is sufficient to use a laser prepulse with the intensity of no less than 4×10^{19} W cm^{-2}. To eject the next-to-last electron of the K shell for producing the Ti^{21+} ion, the laser intensity should be 10^{22} W cm^{-2}, and to obtain the Ti^{22+} ion, the laser intensity should be 1.5×10^{22} W cm^{-2}.

Figure 5 presents the time dependences of γ and the electron momentum components for $\varphi_0 = 0$. As previously, the instant $t = 0$ corresponds to the beginning of the electron acceleration by the laser pulse (instant of ionisation). These dependences corresponds to the initial positions of electrons in the focal plane $\boldsymbol{R}_0 = \{0, 0, z_F\}$ [variant (iv)], $\boldsymbol{R}_0 = \{\lambda/3, 0, z_F\}$ [variant (v)], and $\boldsymbol{R}_0 = \{0, \lambda/3, z_F\}$ [variant (vi)]. Note that variant (iv) differs from variant (i) considered in section 4 by a considerably stronger initial laser field, which acts on the electron at the initial instant of its motion. The calculated ejection angles and energies of electrons are $\psi \approx 30^\circ$, 16°, 8° and $\gamma \approx 10$, 84, 76 for variants (iv), (v), and (vi), respectively. The total acceleration time is approximately the same and is $\sim$100 fs. The energy of the escaped electron in variant (iv) is even somewhat smaller than that in variant (i) (Fig. 3), while the ejection angle is approximately the same despite a strong electric field acting on the electron at $t = 0$. In fact, the initial location of the electron exactly at the laser focus is unfavourable for the selected phase $\varphi_0 = 0$. One can see from Fig. 5 that the electron is accelerated for the time $\sim 2T$ up to the energy corresponding to $\gamma \sim 100$, but then it rapidly loses its energy due to the appearance of a decelerating field. At the same time, the electron energy in variants (v) and (vi) is approximately five times higher than that in variants (ii) and (iii). Correspondingly, the ejection angles are somewhat smaller. Note that the parameters of accelerated electrons depend on their initial position in the vicinity of the focus stronger than in the case discussed in section 4.

The efficiency of acceleration of an electron located initially exactly at the laser focus increases if the initial phase of the field is favourable, which is manifested in the increase in the electron energy and decrease in the ejection angle. Thus, the acceleration efficiency of the escaped electron in the case of the favourable initial phase is several times higher than that for the initially free electron (section 4). For example, for $\varphi_0 = \pi/4$ in variant (iv), we have $\gamma \approx 67$ and $\psi \approx 23^\circ$. For comparison, for $\varphi_0 = \pi/2$, we have $\gamma \approx 36$ и $\psi \approx 27^\circ$. A strong dependence of the parameters of the escaped electron initially located at the laser focus on the initial phase is explained by the tight focusing of laser radiation resulting in the influence of the longitudinal field on the electron motion near the focus. Even if the electron is located initially exactly at the focus, where the longitudinal field is zero, during acceleration it is subjected to the action of the fields depending on the initial phase. Variations in this phase in the case of tight focusing strongly change the acceleration of the electron near the focus. At the same time, when the initial position of the electron is displaced from the axis (within the focal plane) by $\sim\lambda$ and the phase is varied between 0 and 2π, a change in γ is small ($\sim$10 %). This is explained by the rapid escape of electrons from the focal plane.

Calculations performed for different initial positions of the electron on the laser axis and initial phases showed that the energy $\gamma \approx 100$ can be achieved in the case of the optimal initial position of the electron $z_F - z_0 \simeq 1.3\lambda$. Thus, the electron energy in a preionised plasma can be 3–4 times higher than in the case of the acceleration of a free electron (see section 4). By using expressions for the strength and

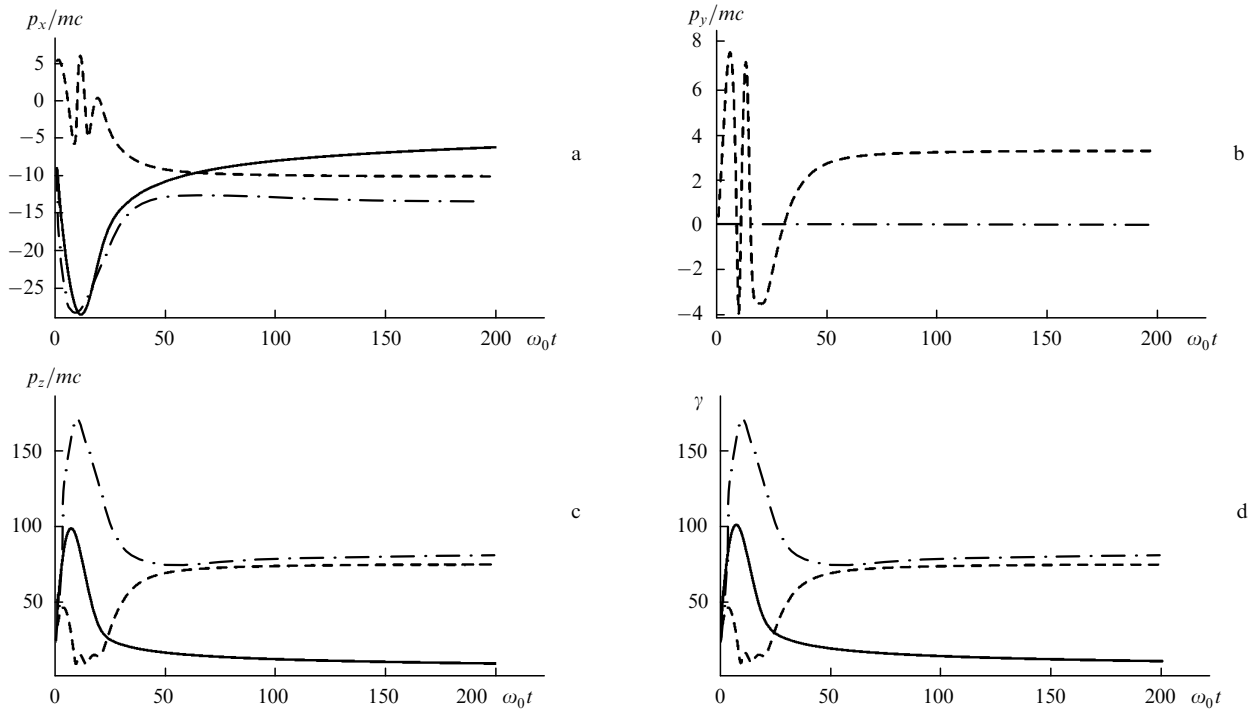

Figure 5. Evolution of the momentum components (a, b, c) and γ (d) for the electron accelerated in a preliminarily ionised plasma for the electron initial positions determined by variants iv–vi and the pulse parameters as in Fig. 3. Solid, dot-and-dash, and dashed curves correspond to variants (iv), (v), and (vi), respectively.

induction of the fields in the paraxial approximation for the focal spot of the same size, we obtain the overestimated (by an order of magnitude) maximal energy of the accelerated electron.

6. Conclusions

Because we were interested first of all in practical results that can be achieved due to a considerable increase in the focal intensity of laser radiation provided by the development of modern laser technologies, we studied in this paper a direct acceleration of a test electron in the case of the tight focusing of laser radiation, when the paraxial approximation cannot be used for the description of the laser field at the focus. The laser field near the focus is described by the solution of Maxwell's equations (16)–(18) obtained for a femtosecond laser pulse under the condition $c\tau \gg \rho(z_F)$ (section 3). We studied the acceleration of an electron initially at rest by a symmetric laser pulse, when the electron was subjected at the initial instant to the field of the leading edge of the pulse (section 4). We also considered the acceleration of an electron produced upon ionisation of a highly charged ion, when the electron is produced and accelerated 'inside' the laser pulse near its maximum (section 5).

Our analysis has shown that upon acceleration of free electrons by a tightly focused laser pulse with the symmetric envelope, they escape at large angles to the laser beam axis. This is explained by the fact that the longitudinal and transverse components of the forces $\boldsymbol{F}_E$ and $\boldsymbol{F}_B$ are of the same order of magnitude. The energy of the escaping electron is much smaller than the energy gained by electrons in the field of a plane electromagnetic wave ($\sim m_e c^2 a^2/2$). In addition, a strict correlation between the electron energy and ejection angle, which is inherent in the acceleration of electrons in the quasi-plane wave approximation, is absent. However, the general tendency is a decrease in the ejection angle with increasing the electron energy. Free electrons located initially near the focus are first accelerated by the leading edge of the pulse and very quickly, during only a few optical cycles, leave the focal region. This occurs before the action of the central, intense part of the pulse on them. As a result, despite the extremely high concentration of the laser energy, the electrons are not accelerated efficiently. In fact, the higher electron energies can be achieved in the case of a moderate focusing, when electrons remained for a longer time in the focal region. This study is of interest for analysis of the operation and applications of modern laser setups using the tight focusing of intense laser pulses [3].

A comparison of the results on the acceleration of an initially free electron by short relativistic laser pulse in exactly defined fields (17) and (18) with the results obtained in the paraxial approximation for the laser field (20) shows that the latter leads to the overestimated value of the maximum energy of accelerated electrons. At the same time, for an ensemble of electrons located near the focus, the number of electrons accelerated up to relativistic energies ($\gamma > 2$) proves to be larger than that in the paraxial approximation. It follows from the calculations that the energy of escaping electrons is maximal when electrons are located in front of the focus at the instant $t = 0$. Our calculations also confirm the conclusion [6] about the quasi-isotropic escape of electrons from the focal region. In particular, this means that the electrons, which were initially located on the axis perpendicular to the polarisation direction, do not move in the plane parallel to the polarisation plane, as was asserted in paper [17], where longitudinal fields were neglected in calculations. Thus, our study confirms the necessity of a correct consideration of longitudinal fields.

According to the idea proposed in [11], we considered the acceleration of photoelectrons from the preliminarily ionised plasma. Unlike [11], we studied the acceleration of electrons in the exactly defined fields rather than 'paraxial' fields. As a whole, as in the case of paraxial fields, our calculations confirm the conclusion that the electron produced upon ionisation acquires a considerably greater energy than the initially free electron. The calculations of the parameters of electrons produced upon ionisation of Ti^{20+} ions confirm the validity of the use of the scheme proposed earlier.

Acknowledgements. The authors thank N.N. Demchenko and Yu.V. Senatskii for useful discussions of the problem and K.V. Popov for numerical test calculations of the tight focusing of laser radiation. This work was supported by the Russian Foundation for Basic Research (Grant No. 06-02-16103) and the ISTC (Grant No. 2289). S.G.B. thanks the Charitable Social Foundation for Support of the Russian Science, the Educational and Scientific Complex of Lebedev Physics Institute, the Program for the Support of Young Scientists of the Presidium of RAS, and the Dynasty Foundation of Non-commercial Programs.

References

1. Schwoerer H., Pfotenhauer S., Jaëckel O. *Nature*, **439**, 445 (2006); Karsch S., Düsterer S., Schwoerer H. *Phys. Rev. Lett.*, **91**, 015001 (2003).
2. Albert O., Wang H., Liu D., et al. *Opt. Lett.*, **25**, 1125 (2000).
3. Bahk S.-W., Rousseau P., Planchoun T.A. *Opt. Lett.*, **29**, 2837 (2004).
4. Hartemann F.V., Fochs S.N., LeSage G.P., et al. *Phys. Rev. E*, **51**, 4833 (1995).
5. Esarey E., Sprangle P., Krall J. *Phys. Rev. E*, **52**, 5443 (1995).
6. Quesnel B., Mora M. *Phys. Rev. E*, **58**, 3719 (1998).
7. Narozny N.B., Fofanov M.S. *Zh. Eksp. Teor. Fiz.*, **117**, 86 (2000); Narozhny N.B., Fofanov M.S. *Phys. Lett. A*, **295**, 87 (2002).
8. Stupakov G.V., Zolotorev M.S. *Phys. Rev. Lett.*, **86**, 5274 (2001).
9. Wang P.X., Ho Y.K., Yuan X.Q., et al. *Appl. Phys.*, **91**, 856 (2002).
10. Salamin Y.I., Keitel C.H. *Phys. Rev. Lett.*, **88**, 095005 (2002).
11. Hu S.X., Starace A.F. *Phys. Rev. Lett.*, **88**, 245003 (2002); *Phys. Rev. E*, **73**, 066502 (2006).
12. Maltsev A., Ditmire T. *Phys. Rev. Lett.*, **90**, 053002 (2003).
13. Bahari A., Taranukhin V.D. *Kvantovaya Elektron.*, **33**, 563 (2003); **34**, 129 (2004) [*Quqntum Electron.*, **33**, 563 (2003); **34**, 129 (2004)].
14. Masuda S., Kando M., Kotaki H. *Phys. Plasmas*, **12**, 013102 (2005).
15. Wang W., Wang P.X., Ho Y.K., et al. *Europhys. Lett.*, **73**, 211 (2006).
16. Malka G., Miquel J.L. *Phys. Rev. Lett.*, **77**, 75 (1996).
17. Malka G., Lefebvre E., Miquel J.L. *Phys. Rev. Lett.*, **78**, 3314 (1997).
18. Moore C.I., Ting A., McNaught S.J., et al. *Phys. Rev. Lett.*, **82**, 1688 (1999).
19. Akhmanov S.A., Nikitin S.Yu. *Fizicheskaya optika* (Physical Optics) (Moscow: Moscow State University, 1998).
20. Davis L.W. *Phys. Rev. A*, **19**, 1177 (1979).
21. Agrawal G.P., Pattanayak D.N. *J. Opt. Soc. Am.*, **69**, 575 (1979).
22. Barton J.P., Alexander D.R. *J. Appl. Phys.*, **66**, 2800 (1989).

23. Cicchitelli L., Hora H., Postle R. *Phys. Rev. A*, **41**, 3727 (1990).
24. Duan K., Wang B., Lü B. *J. Opt. Soc. Am. A*, **22**, 1976 (2005).
25. Bahk S.-W., Rousseau P., Planchoun T.A. *Appl. Phys. B*, **80**, 823 (2005).
26. Landau L.D., Lifshits E.M. *The Theory of Fields* (London: Pergamon Press, 1971; Moscow: Nauka, 1988).
27. Lawson J.D. *IEEE Trans. Nucl. Sci.*, **NS-26**, 4217 (1979); Woodward P.M. *J. Inst. Electr. Eng.* **93**, 1554 (1947).
28. Wang J.X., Scheid W., Hoelss M., et al. *Phys. Rev. E*, **65**, 028501 (2002).
29. Mora P., Quesnel B. *Phys. Rev. Lett.*, **80**, 1351 (1998).
30. Cheng Ya, Xu Zhizhan. *Appl. Phys. Lett.*, **74**, 2116 (1999).
31. Rau B., Tajima T., Hojo H. *Phys. Rev. Lett.*, **78**, 3310 (1997).
32. Milant'ev V.P., Shaar Ya.N. *Zh. Tekh. Fiz.*, **70**, 100 (2000).
33. Born M., Wolf E. *Principles of Optics*, 4th ed. (Oxford: Pergamon Press, 1969; Moscow: Nauka, 1973).
34. Greene P.L., Hall D.G. *Opt. Express*, **10**, 411 (1999).
35. http:library.wolfram.com/.
36. He X., Li R.X. *Phys. Plasmas*, **12**, 073101 (2005).
37. Amosov M.V., Delone N.B., Krainov V.P. *Zh. Eksp. Teor. Fiz.*, **91**, 2008 (1986).